Synergistic Enhancement of Anti-aging and Fatigue Properties of Graphene/Rubber Powder Composite Modified Asphalt

Yunpeng SHANG *

G211 Nanluo Project Office, Gansu Jiaojian Project Management Co., Ltd., Lanzhou 730000, Gansu, China

http://doi.org/10.5755/j02.ms.41790

Received 4 June 2025; accepted 17 July 2025

Traditional modified asphalt has limitations in anti-aging, fatigue resistance, and environmental protection performance. In this study, a new type of graphene/rubber powder composite modified asphalt (CMA) is prepared to synergistically enhance the anti-aging and anti-fatigue properties. CMA is prepared by melting and co-mixing at 180 ℃ and high-speed shearing at 5000 rpm. The performance is evaluated using scanning electron microscopy (SEM), dynamic shear rheometer (DSR), and Fourier transform infrared spectroscopy (FTIR) in the experiment. The results showed that the modified asphalt showed excellent anti-aging performance. After 60 hours of aging, the phase angle only decreased from 60.1° to 56.4°, while the phase angle of the unmodified matrix asphalt group decreased from 50.1° to 40.3°. The smaller the decrease of phase angle, the better the aging resistance of asphalt. The anti-aging performance of the modified asphalt was about 62.2% higher than that of the base asphalt. The aging index of carbonyl and sulfoxide groups significantly decreased (0.035 and 0.037, respectively). The anti-fatigue performance has also been significantly improved, with the CMA reaching 113,652 cycles at 2.5 % strain, an increase of 73.98 % compared to the matrix asphalt group. This mechanism was attributed to the layered barrier structure of graphene (delaying oxidation) and the sulfur crosslinked network of rubber powder (absorbing thermal stress). At the same time, the rigid structure of graphene combined with the flexibility of rubber formed an interlocking network that resisted crack propagation and could suppress the propagation of asphalt microcracks. Such a structure can effectively improve the anti-aging and anti-fatigue performance of modified asphalt, providing a promising solution for the design of long-life pavement, especially in heavy traffic and extreme climate environment.
Keywords: graphene, rubber powder, asphalt, anti-aging performance, fatigue resistance performance.

1. INTRODUCTION

With the continuous development of transportation infrastructure construction, the demand for high-performance asphalt materials is increasing day by day. The limitations of traditional modified asphalt in anti-aging, fatigue resistance, environmental protection, and other aspects are gradually highlighted, and it is difficult to meet the high-performance requirements of modern traffic for pavement materials [1]. Modern transportation presents the characteristics of high density, large tonnage, and speed. The frequent passage of heavy vehicles imposes enormous loads on the road surface, leading to accelerated fatigue damage. In addition, the increase in traffic flow also puts the service life of the road surface to a severe test [2]. According to statistics, for every doubling of traffic volume, the service life of the road surface will be shortened by half. In addition to the impact of traffic loads, environmental factors have also caused serious damage to asphalt pavements. Natural factors such as ultraviolet radiation, temperature changes, and rainwater erosion accelerate the aging process of asphalt [3]. The performance of aged asphalt significantly decreases, manifested as increased viscosity, decreased toughness, and increased brittleness, ultimately leading to pavement cracking, peeling, and potholes. Therefore, it is of great practical significance to develop new modified asphalt materials with excellent anti-aging and anti-fatigue properties [4]. At present, many scholars have also achieved certain research results in graphene and rubber powder modified asphalt.

Yang et al. addressed the shortcomings of traditional asphalt in terms of high-temperature stability, resistance to permanent deformation, and dispersibility of polymer modifiers. They used a titanate coupling agent to wet modify heavy calcium carbonate. This method prepared calcium carbonate coupled with titanate, and then blended with styrene butadiene styrene to modify asphalt, resulting in composite modified asphalt (CMA). The CMA prepared by this method exhibited better high-temperature stability, resistance to permanent deformation, and compatibility with polymer modifiers [5]. Yan et al. added nano titanium dioxide and graphene to asphalt, and improved the performance of asphalt through mutual synergy [6]. Li et al. addressed the issue of road surface aging under environmental factors such as temperature and light, and prepared CMA of nano $CaCO_3$/nano ZnO/styrene butadiene rubber (SBR) using 6 % KH-550 activated nano $CaCO_3$ surface and 6% aluminate activated nano ZnO surface. The optimal ratio of CMA was 4 % nano $CaCO_3$ + 5 % nano ZnO + 4 % SBR. Under this ratio, the aging performance of CMA decreased by 6.9%, and the viscosity increased by 14.6 % – 23.1 % [7]. Wen et al. proposed a composite modification of petroleum asphalt using rock asphalt, other modifiers, and crushed rubber (CR) to address the shortcomings of traditional petroleum asphalt in terms of fatigue life and performance degradation after

* Corresponding author: Y. Shang
E-mail: *ShangYunpeng@GSCPMCL.ORG.CN*

aging. Reducing the content of rock asphalt and increasing the content of rubber powder could significantly improve the fatigue resistance of styrene butadiene styrene (SBS)/CR CMA, extending its fatigue life by more than 5 times [8]. In a word, although the schemes of Yang S., Yan K. and Li Z. have improved the high-temperature stability or aging resistance of asphalt to varying degrees, they have failed to effectively solve the problem of fatigue resistance, leading to hidden dangers in the durability of modified asphalt under long-term cyclic load. Although Wen Y's scheme significantly extends fatigue life, it ignores the synchronous optimization of anti-aging performance, which is difficult to resist the potential weakening of environmental aging on fatigue performance. And these studies have not explored the synergistic enhancement mechanism between fatigue resistance and anti-aging (anti-oxidation) performance.

The above research results are far from sufficient to improve the performance of asphalt and meet the needs of existing transportation infrastructure construction. Therefore, experts and scholars have focused on the anti-aging and fatigue properties of asphalt. Wang et al. found that graphene oxide can significantly improve the high temperature stability and aging resistance of asphalt. The layered structure of graphene oxide could form a physical shielding layer in asphalt, effectively blocking the invasion of oxygen and ultraviolet rays, thereby delaying the aging process of asphalt [9]. This study proved the benefits of graphene oxide in anti-aging, but did not further explore the synergistic effect of combining graphene oxide with rubber powder. Yin et al. found that rubber powder could improve the elasticity and toughness of asphalt, and enhance its fatigue resistance. The sulfur crosslinked network in rubber powder could absorb thermal stress fluctuations, disperse stress concentration, and suppress the propagation of microcracks [10]. This study demonstrated the role of rubber powder in improving fatigue resistance, but did not address the performance issue of long-term aging. Si et al. found that graphene nanoflakes can enhance the mechanical properties and anti-aging properties of asphalt. The high specific surface area and good dispersibility of graphene nanosheets could form strong interfacial bonding with the asphalt matrix, improving the overall performance of asphalt [11]. Although this study found that graphene nanoflakes can enhance the mechanical properties and anti-aging properties of asphalt, it did not further explore how to improve the fatigue resistance of asphalt. Hoang et al. proposed using a combination of graphene oxide and styrene butadiene styrene block copolymer CMA to prepare graphene oxide/SBR CMA with different dosages. Graphene oxide/SBR CMA had stronger high-temperature deformation resistance compared to SBR modified asphalt alone. When the content of graphene oxide was 0.4%, the rutting factor and shear modulus reached their maximum values, and the effect was most significant [12]. However, the research mainly focused on the high temperature deformation resistance, and there was little research on how to improve the aging resistance and fatigue resistance of asphalt at the same time.

In summary, graphene has a unique 2D nanosheet structure and excellent physical and chemical properties, while rubber powder has good elastic buffering properties. The composite of graphene and rubber powder is used to modify asphalt, combining the nano reinforcement effect of graphene and the elastic buffer advantage of rubber powder, which is expected to significantly improve the aging and fatigue resistance of asphalt. However, existing research has focused on the impact of a single material on asphalt performance, and the study of the synergistic mechanism of Graphene/Rubber Powder Composite Modified Asphalt (hereinafter referred to as G/RPCMA) is not yet in-depth [13]. In terms of the preparation process, existing methods have problems such as uneven dispersion of graphene, weak bonding with rubber powder and asphalt matrix, which make it difficult to achieve the optimal performance of CMA [14]. Given this, this study proposes a G/RPCMA preparation scheme, which aims to significantly improve the aging and fatigue resistance of existing asphalt.

The innovation of the research first lies in the proposed dual effect synergistic anti-aging mechanism of "external shielding+internal buffering". The two-dimensional lamellar structure of graphene by Hummer’s method is used to form a parallel physical barrier in asphalt, which effectively blocks the penetration of external aging factors. At the same time, the sulfur cross-linked network of rubber powder absorbs thermal stress fluctuations, and delays the oxidative embrittlement of asphalt. The synergistic effect of the two significantly improves the anti-aging performance. Secondly, a "rigid flexible interlocking" anti-fatigue structure was constructed, in which graphene enhances the elastic recovery ability of the asphalt matrix, rubber powder particles act as flexible stress absorption points to suppress microcrack propagation, and sulfur bonds at the interface work synergistically with van der Waals forces to significantly improve fatigue life. In the preparation process of graphene, the characteristics of graphene were optimized through low-temperature pre oxidation and step heating oxidation processes, resulting in high graphitization degree and abundant surface defects. At the same time, the compatibility with asphalt was improved, achieving uniform dispersion and suppressing the diffusion of aging components. In terms of composite modification process and formulation, a step-by-step feeding and shearing process is adopted to achieve micrometer level dispersion of components, promote interfacial interactions, and balance the "shielding buffering toughening" function through collaborative design.

2. EXPERIMENTAL MATERIALS AND METHODS

Table 1 provides details of the equipment and materials required for preparing G/RPCMA. Research has shown that graphene can form parallel physical shielding layers in asphalt through its 2D nanosheet structure, effectively blocking the penetration of oxygen, moisture, and ultraviolet radiation, and inhibiting free radical chain reactions [15]. Similarly, the sulfur cross-linked network in rubber powder is known to absorb thermal stress fluctuations through elastic deformation, which can delay the oxidation embrittlement of asphalt [10]. The dual anti-aging system of "external shielding + internal buffering" constructed by combining the two can synergistically improve the anti-aging performance of CMA.

Table 1. Required materials and equipment

Raw material		
Name	Parameter	Manufacturer
Asphalt	Penetration 60 – 80 (0.1 mm)	China Petroleum & Chemical
Waste rubber	80 mesh tire rubber powder	Green Source Rubber Recycling Co., Ltd
SBS modifier	YH-791	Yueyang Petrochemical Co., Ltd
Epoxy stabilizer	Purity 99.5 %	
Graphite	Fixed carbon ≥ 99 %	Qingdao Heilong Graphite Co., Ltd
98 % concentrated sulfuric acid	Analytical pure (AR)	Guoyao Chemical Reagent Co., Ltd
85 % phosphoric acid		
Sodium nitrate		
Potassium permanganate		
Deionized water		
Equipment		
Name	Type	Manufacturer
Electronic balance	BSA224S-CW	Sartorius
High speed shear disperser	GMSD2000/4	Shanghai Sijun Machinery Equipment Co., Ltd
High temperature vacuum drying oven	DZF-6050	Shanghai Yiheng Scientific Instrument Co., Ltd
Ice bath distiller	JZ-2000	Shanghai Yiheng Scientific Instrument Co., Ltd
Fourier transform infrared spectroscopy (FTIR)	Nicolet iS50	Thermo Fisher Scientific
X-ray diffractometer (XRD)	TD-5000	Dandong Tongda Technology Co., Ltd
Raman spectrometer	DXR™3xi	Thermo Fisher Scientific
Dynamic shear rheometer (DSR)	RT-DSR150	Shanghai Jinshan Souai Procurement Platform Supplier

In the anti-fatigue mechanism, the nano reinforcement effect of graphene can significantly enhance the elastic recovery ability of asphalt matrix and reduce viscous deformation.

Rubber powder disperses stress concentration through flexible particles, suppressing the propagation of microcracks. The interface between the two forms a "rigid flexible interlocking" structure through the combination of sulfur bonds and van der Waals forces, which can synergistically reduce fatigue factors. Therefore, based on the existing technology, this research uses the materials and equipment provided above to prepare CMA with excellent aging resistance and fatigue performance. The preparation process is shown in Fig. 1.

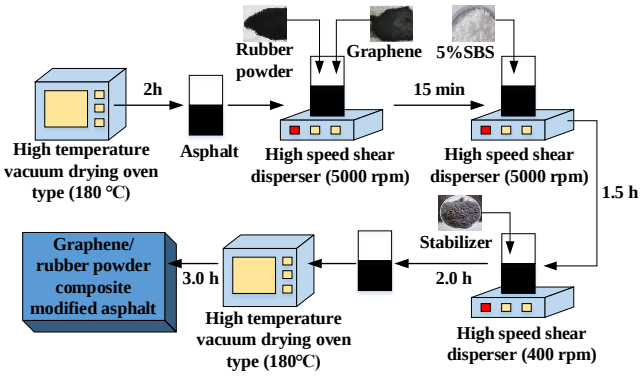

Fig. 1. Preparation process of G/RPCMA

In Fig. 1, firstly, the matrix asphalt is melted at high temperature. The matrix asphalt sample is heated to 180 ℃ in a DZF-6050 high-temperature vacuum drying oven and maintained for 2 hours to completely transform into a flowing liquid state. Subsequently, the graphene dispersion is added to the liquid matrix asphalt at a mass ratio of 1 wt.% of the matrix asphalt (Graphene, as a nanofiller, can achieve a layer barrier effect with a 1 % addition in amount, while excessive addition can lead to agglomeration and reduce performance). While rubber powder at a mass ratio of 0.1 wt.% of the matrix asphalt is added (Rubber powder, due to its high volume expansion characteristics, can be added in an amount of 1 % to meet the demand). The GMSD2000/4 high-speed shear disperser is used to shear at a speed of 5000 rpm for 15 minutes to achieve uniform dispersion. Next, SBS modifier with a mass of 5 % of the base asphalt is added and sheared at 5000 rpm for 1.5 hours to further refine the SBS modifier and rubber powder to the micrometer level (SBS, as a polymer modifier, has an industry recognized effective modification threshold of 5 %. Below this concentration, it cannot form a "sea island structure" that runs through the network), promoting their development and swelling in the asphalt matrix. Afterwards, 1 g of epoxy stabilizer is added and the rotation speed is adjusted to 400 rpm. Shear is continued for 2 hours to enhance the stability of the system. After completing the above mixing and shearing processes, the mixed product is placed again in the DZF-6050 high-temperature vacuum drying oven. Under the condition of 180 ℃, it is maintained for 3 hours to further promote the interaction between the modifier and the asphalt matrix, optimize the performance of the modified asphalt, and obtain G/RPCMA. The graphene in the above steps is prepared using the Hummers method, as shown in Fig. 2. In Fig. 2, first, 98 % concentrated sulfuric acid and 85 % phosphoric acid are mixed in a volume ratio of 9:1 and placed in a JZ-2000 ice bath distiller for pre-cooling to below 4 ℃ to reduce the occurrence of side reactions. Under stirring conditions, 2 g of graphite powder, 1 g of sodium nitrate, and 6 g of potassium permanganate are sequentially added to the mixed acid, while maintaining the ice bath temperature at 4 ℃ to avoid uncontrolled reaction caused by intense heat release. The mixture was continuously stirred in an ice bath distiller for 2 hours to allow the sulfuric acid molecules to fully intercalate into the graphite, forming a pre-oxidized intermediate. Subsequently, the temperature is slowly raised to 35 ℃ – 38 ℃, and stirring is continued for 6 hours to extend the oxidation time and enhance the deep oxidation of graphite.

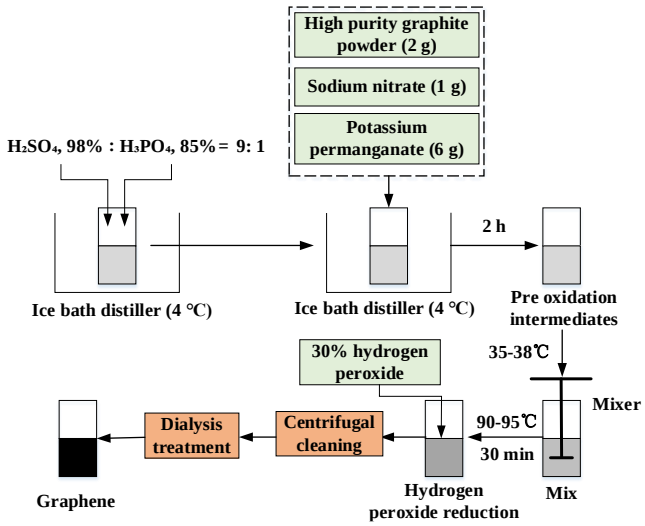

Fig. 2. Preparation process of graphene based on Hummer's method

Afterwards, deionized water is slowly added, and the temperature is raised to 90 – 95 ℃. The reaction is carried out at this temperature for 30 minutes, promoting the hydrolysis of interlayer compounds and forming oxidized graphite. Then, 30 % hydrogen peroxide is added to reduce the residual MnO_2 to Mn^{2+}. Subsequently, 5 % dilute hydrochloric acid and deionized water are centrifuged multiple times (at a speed of 10,000 rpm) until the filtrate is free of SO_4^{2-}. Finally, the product is loaded into a dialysis bag with a cut-off molecular weight of 8 – 14 kDa and dialyzed continuously for 3 weeks to completely remove metal ions and residual acids, thereby obtaining high-purity oxidized graphite.

In order to verify whether the G/RPCMA obtained by the above preparation process has successfully achieved the expected anti-aging synergistic effect and anti-fatigue structure, and to quantitatively evaluate the advantages of its aging resistance and fatigue performance, it is necessary to characterize and test the material. The specific G/RPCMA detection method for research preparation is shown in Fig. 3.

Firstly, in detection by scanning electron microscope, the dried G/RPCMA is uniformly dispersed in solvents such as ethanol and coated with a platinum conductive film to improve conductivity and then installed on the scanning electron microscope sample stage. The acceleration voltage of the instrument is 4 KV, the working distance is 1 mm, and the electron beam current is 100 pA. The sample surface is scanned point by point by a secondary electron detector and the signal is recorded to form an image. Finally, image analysis software is utilized to analyze the characteristics of powder particles such as size, shape, distribution, and surface morphology, while recording data and generating reports.

In detection by XRD, the G/RPCMA sample is ground into a fine powder to ensure the clarity and accuracy of diffraction peaks. Then, a sample clamp is used to fix the G/RPCMA powder sample onto the sample holder, ensuring that the sample was centered and parallel to the holder. Next, a Cu target is selected as the radiation source with a wavelength of 1.5406 Å. The range of XRD diffraction angle 2θ is 10 ~ 80°, the step size is adjusted to 0.01°, the scanning speed is 5 °/min, and the voltage and current of the X-ray tube are 110 kV and 50 mA.

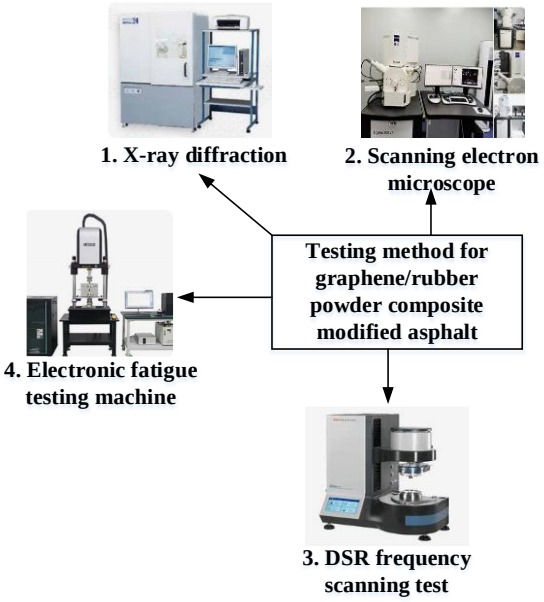

Fig. 3. G/RPCMA detection chart

After setting the above measurement conditions on the software interface, click start. The instrument can start sending X-rays and recording diffraction signals [16 – 18].

The anti-aging test is divided into short-term aging test and long-term test. The G/RPCMA sample is placed in a glass bottle with a volume of 225 cm^3, and subjected to short-term aging simulation for 1 hour and pressure aging containers for different times (0, 15, 30, 45, 60 hours) under the conditions of 163 ℃, air flow, and rotation. Afterwards, a DSR is used for DSR frequency scanning test to determine the $G - R$ constant of asphalt, as shown in Eq. 1.

$$G - R = \frac{G^* \times \cos^2 \delta}{\sin \delta}, \tag{1}$$

where G^* is the complex shear modulus of asphalt; δ is the phase angle. The larger the $H - F$ value, the more brittle and prone to cracking the asphalt. Subsequently, Nicolet iS50 FTIR Spectrometer is used to analyze the polarity changes of carbonyl (IC=O) and sulfoxide (IS=O) groups in modified asphalt samples before and after the rotating thin film oven test (RTFOT). After short-term aging, the samples are placed in a pressurized aging vessel (PAV) and subjected to conditions of 100 ℃, 2.1 MPa air pressure, and a duration of 20 hours to simulate the long-term thermal oxidative aging process in a natural environment for 5 – 10 years. After aging, the aged asphalt sample is taken out from the PAV and allowed to cool to room temperature for penetration and softening point testing.

3. RESULT ANALYSIS

3.1. Microstructure analysis of graphene

Fig. 4 shows the results of observing the physical microstructure and structural details of commonly used graphene and graphene prepared by the Hummer's method using a scanning electron microscope (SEM). Fig. 4 a shows

the SEM image of graphene prepared by Hummer's method, which exhibits a typical layered structure with abundant wrinkles and defects on the surface of the layers.

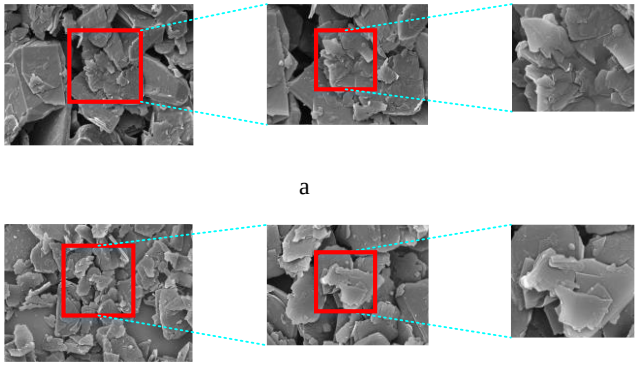

a

b

Fig. 4. SEM images of two types of graphene: a – graphene prepared by the Hummer's method; b – common graphene

This structure can enhance the interfacial bonding strength with the asphalt matrix. In addition, the graphene has a relatively thin layer thickness (usually 1-3 layers) and a large specific surface area. It can form a uniform intercalation structure in asphalt, effectively adsorb light components in asphalt and restrict their flow, thereby suppressing molecular chain breakage and oxidation reaction diffusion during the aging process. Fig. 4 b shows the SEM image of common graphene. The structure is smoother and denser, with obvious layer stacking and fewer surface functional groups. Although this structure has excellent electrical conductivity and mechanical properties, it has poor compatibility with asphalt and is prone to agglomeration, resulting in limited dispersion and anti-aging properties of modified asphalt.

Fig. 5 uses TD-5000 XRD and DXR™3xi Raman spectrometer to detect commonly used graphene, as well as using the Hummers method to detect the prepared graphene. Fig. 5 a shows the XRD spectra of two types of graphene. These two types of graphene have a high peak at 29.5°, indicating that both types of graphene have a graphitized structure. The graphene prepared by the study also shows higher peaks at 53.4° and 64.1°, indicating a higher degree of graphitization. Fig. 5 b shows the Raman spectra of two types of graphene. Commonly used graphene and prepared graphene exhibit high 2D harmonic peaks at 10.5×10^3 cm^{-1} and 10.5×10^3 cm^{-1}, indicating that both types of graphene have highly graphitized structures. Graphene prepared by the Hummer's method exhibits a more regular arrangement of carbon atoms due to its higher degree of graphitization. In asphalt, it can form an effective reinforcement network, disperse stress, reduce stress concentration, and improve the fatigue performance of asphalt.

3.2. Evaluation of aging resistance of asphalt

Base asphalt is defined as sample 1; The commonly used modified asphalt prepared from graphene is sample 2; The modified asphalt prepared using graphene and rubber powder is sample 3. The evaluation scheme of asphalt aging resistance is mainly realized through the frequency scanning test of DSR and FTIR test.

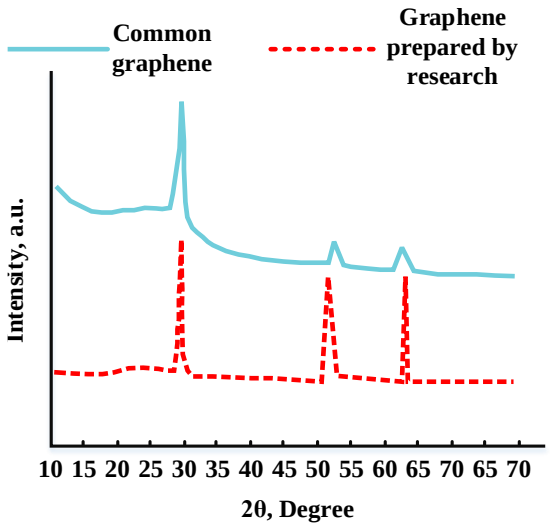

a

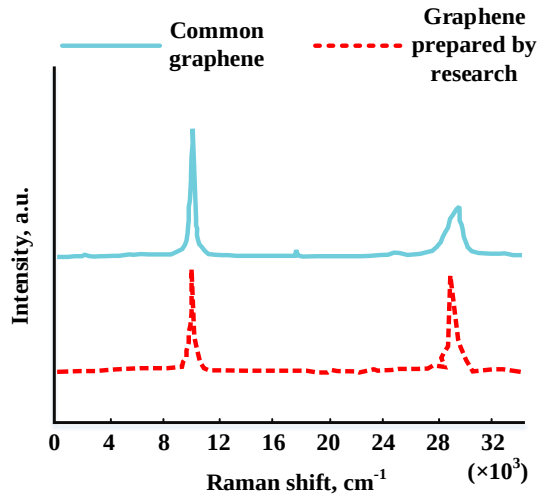

b

Fig. 5. XRD and Raman spectra of two types of graphene: a – XRD spectra; b – Raman spectra

In the frequency scanning test of the DSR, the $G-R$ constant of three asphalt samples at different aging times is calculated and a black space diagram is drawn to evaluate the aging resistance of asphalt, as shown in Fig. 6. In Fig. 6 a, after 60 hours of aging, the phase angle of sample 1 decreases from 50.1° to 40.3°, which indicates that its elasticity decreases significantly, its viscosity increases, and its anti-aging performance is poor. In Fig. 6 b, sample 2 shows a decrease in phase angle from 55.2° to 43.8° under the same aging time. Although the decrease in phase angle is smaller than that of sample 1, it still exhibits a certain aging trend. In Fig. 6 c, after aging for 60 hours, the phase angle of asphalt sample 3 only decreases from 60.1° to 56.4°, with a significantly smaller decrease compared to the first two types of asphalt. This shows that the prepared G/RPCMA has good anti-aging ability. The reason is that studying the preparation of graphene can better prolong the permeation path of oxygen and slow down the oxidation reaction of asphalt. The addition of rubber powder improves the elasticity and toughness of asphalt, enabling it to better maintain its performance during aging. The results of penetration and softening point tests are shown in Fig. 7.

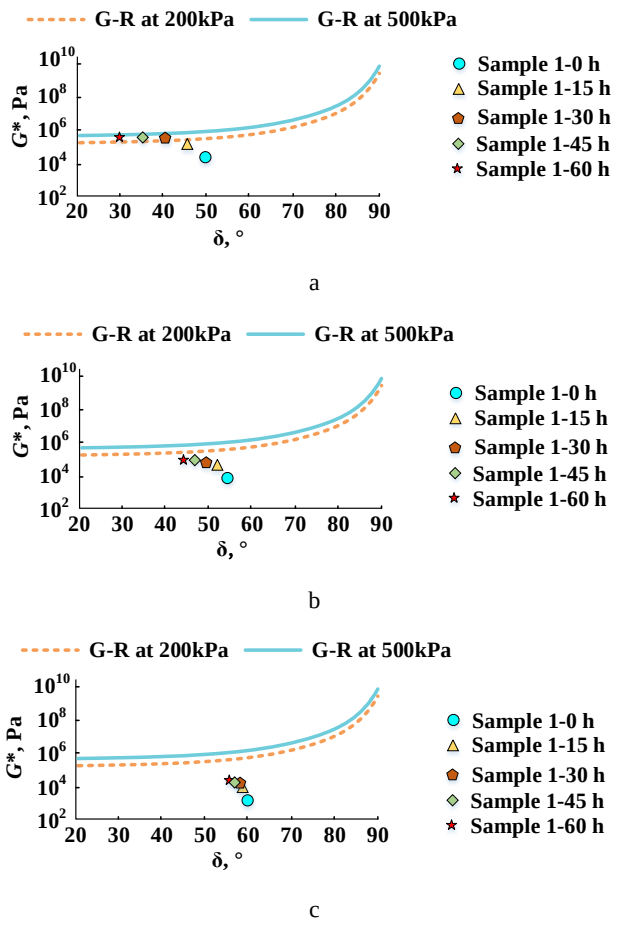

Fig. 6. Black spatial images of three types of asphalt samples: a – asphalt sample 1; b – asphalt sample 2; c – asphalt sample 3

In Fig. 7 a, sample 3 has a needle penetration of 7.2 mm before PAV aging, which decreased to 55 mm after long-term thermal oxidative aging, with a needle penetration retention rate of 76.4 %. This value is significantly higher than the other two groups, indicating that graphene and rubber powder effectively inhibit the thermal oxidation fracture of asphalt molecular chains through interfacial cross-linking, thereby delaying the hardening process. In Fig. 7 b, sample 3 has an initial softening point of 58.2 ℃, which only increased to 63.5 ℃ after PAV aging, with a temperature rise of 5.3 ℃, a decrease of 31.2 % and 15.9 % compared to unmodified asphalt (ΔT = + 7.7 ℃) and single graphene modified asphalt (ΔT = + 6.3 ℃). This minimal temperature variation confirms that the composite modified system can stabilize the asphalt colloid structure. Its 3D network synergistically enhances the durability of the material's resistance to high-temperature deformation through the elastic buffering of rubber powder and the barrier effect of graphene. The FTIR and aging indices of carbonyl and sulfoxide groups for three types of asphalt samples are shown in Fig. 8.

In Fig. 8 a, the FTIR of asphalt sample 1 – sample 3 shows significant enhancement in the characteristic peak intensities at 1700 cm^{-1} and 1030 cm^{-1}. This indicates that during the aging process, these asphalt samples undergo oxidation reactions, generating compounds containing carbonyl and sulfoxide groups.

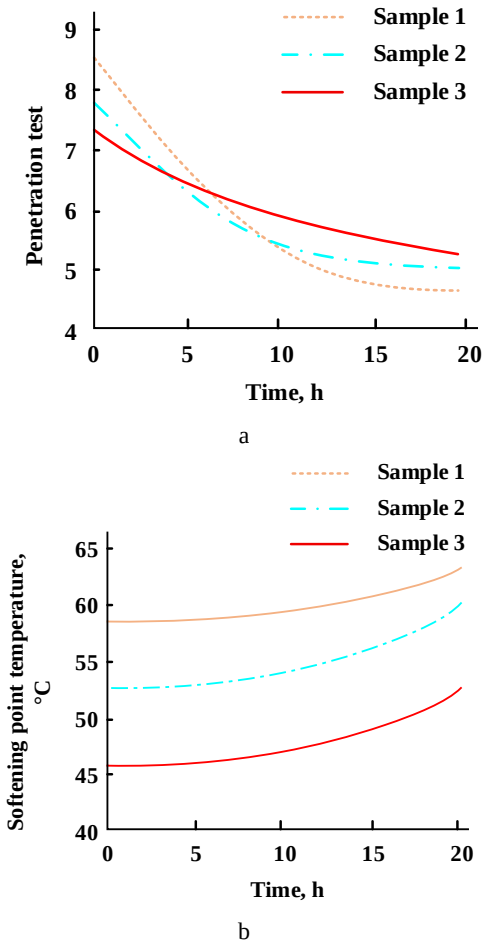

Fig. 7. Penetration and softening point tests of three asphalt samples: a – penetration test; b – softening point test

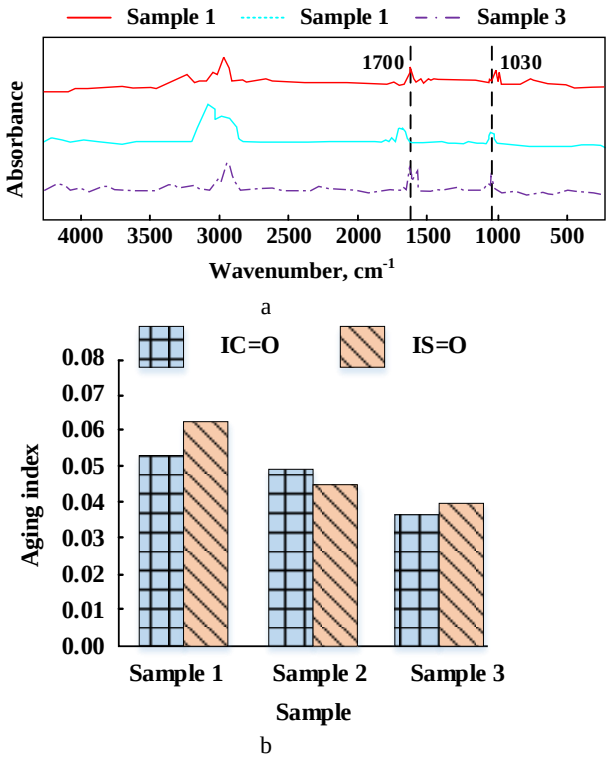

Fig. 8. FTIR and aging indices of carbonyl and sulfoxide groups for three asphalt samples: a – FTIR; b – aging index of carbonyl and sulfoxide groups

In Fig. 8 b, the aging indices of carbonyl and sulfoxide groups in sample 1 are approximately 0.051 and 0.062. The aging indices of carbonyl and sulfoxide groups in sample 2 are approximately 0.049 and 0.043. The aging indices of carbonyl and sulfoxide groups in sample 3 are approximately 0.035 and 0.037. This shows that the prepared modified asphalt sample can improve the aging resistance very well. Table 2 shows the viscosity of different asphalts before and after thermal oxidative aging.

Table 2. Viscosity values of different asphalt before and after thermal oxidative aging

Asphalt type	Time, h	Viscosity number $\times 10^3$ Pa·s	Time, h	Viscosity number $\times 10^3$ Pa·s	Time, h	Viscosity number $\times 10^3$ Pa·s
sample 1	0	3.14	15	2.96	45	2.52
			30	2.73	60	2.21
sample 2	0	2.14	15	2.02	45	1.81
			30	1.90	60	1.76
sample 3	0	1.63	15	1.53	45	1.39
			30	1.45	60	1.31

In Table 2, with the increase of thermal oxidative aging time, the viscosity values of the three asphalt samples show a decreasing trend. The viscosity of sample 1 decreases from the initial 3.14×10^3 Pa·s to 2.21×10^3 Pa·s after 60 hours. The viscosity of sample 2 decreases from 2.14×10^3 Pa·s to 1.76×10^3 Pa·s. The viscosity of sample 3 decreases from 1.63×10^3 Pa·s to 1.31×10^3 Pa·s. This indicates that during the thermal oxidative aging process, the viscosity of asphalt gradually decreases, which may be due to the molecular structure changes caused by the volatilization or oxidation reactions of light components in asphalt. In contrast, the viscosity of sample 3 has the smallest decline, indicating that it has better stability and the best anti-aging performance during thermal oxygen aging.

3.3. Evaluation of fatigue resistance of asphalt

Three samples are subjected to frequency scanning tests at strain levels of 2.5 %, 5.0 %, 7.5 %, and 10 %. At each strain level, the sample is scanned at a frequency of 50 Hz, and the complex modulus and phase angle are recorded at different frequencies, as shown in Table 3.

Table 3. Complex modulus and phase angle of samples at different strain levels

Asphalt type	Strain level, %	Complex modulus, kPa	Phase angle, °
sample 1	2.5	32	50.1
	5.0	45	46.2
	7.5	63	43.8
	10	79	41.3
sample 2	2.5	12	55.2
	5.0	19	53.2
	7.5	21	51.3
	10	29	50.8
sample 3	2.5	0.9	60.1
	5.0	10	58.9
	7.5	16	57.6
	10	29	55.2

In Table 3, there are significant differences in the complex modulus and phase angle of the three asphalt samples at different strain levels. The complex modulus of Sample 1 significantly increases with increasing strain level, from 32 kPa at 2.5 % strain to 79 kPa at 10 % strain. This indicates that its deformation resistance is enhanced under high strain, but the phase angle gradually decreases from 50.1° to 41.3°, indicating a relative increase in viscosity. The complex modulus of sample 2 changes relatively smoothly, increasing from 12 kPa to 29 kPa, and the phase angle decreases from 55.2° to 50.8°, demonstrating good viscoelastic equilibrium. The complex modulus of sample 3 is the lowest, increasing from 0.9 kPa to 29 kPa, and the phase angle decreases from 60.1° to 55.2°, indicating that it is softer and more elastic in its initial state. This indicates that sample 3 has better adaptability and elasticity under low strain, and can more effectively absorb and disperse stress, thereby reducing the accumulation of fatigue damage. In practical applications, this characteristic helps to improve the fatigue resistance of road surfaces and extend their service life. The number of cycles of fatigue failure at different strain levels for the three samples is shown in Fig. 9. In Fig. 9, as the strain level increases, the number of fatigue failure cycles for all three asphalt samples shows a decreasing trend. The specific analysis is as follows: Sample 1 has 65,323 cycles at a strain level of 2.5 %, and as the strain level increases to 10%, the number of cycles decreases to 5,632. Under the same conditions, the number of cycles for sample 2 decreases from 89,652 to 7,652. Sample 3 decreases from 113,652 to 8,652. The fatigue life attenuation rates of the three groups of samples are similar (91.4 % – 92.4 %). Overall, sample 3 exhibits the highest number of cycles at all strain levels. This indicates that it has stronger anti-fatigue performance and can maintain more lasting stability under high strain and frequent load, making it a better choice for anti-fatigue materials. This characteristic enables it to effectively delay crack propagation in engineering scenarios such as bridge joints and airport runways that are subjected to high-frequency dynamic loads.

3.4. Discussion

Graphene prepared by the Hummer‘s method exhibits layered folds and defect structures compared to conventional graphene. This structural characteristic significantly increases its specific surface area and surface functional group density, thereby enhancing its interfacial bonding with the asphalt matrix. The study by Yu et al. showed that the wrinkled structure and oxygen-containing functional groups of graphene can adsorb light components in asphalt through van der Waals forces and hydrogen bonding, inhibiting their volatilization and oxidation during aging [19]. At the microscopic level, the unique two-dimensional graphene layer structure of graphene has the characteristics of high crystallinity and large specific surface area. This structure greatly prolongs the diffusion path of oxygen molecules and ultraviolet photons into the interior of asphalt, and effectively blocks direct contact between external aging factors and active components of asphalt, delaying the initiation of oxidation chain reactions and the diffusion of free radicals from the source. At the same time, the three-dimensional elastic network structure of rubber powder, with its excellent flexibility and high elasticity, can efficiently absorb and dissipate internal stress

fluctuations caused by thermal expansion, oxidative shrinkage, or external loads through the stretching, curling, and conformational changes of molecular chains.

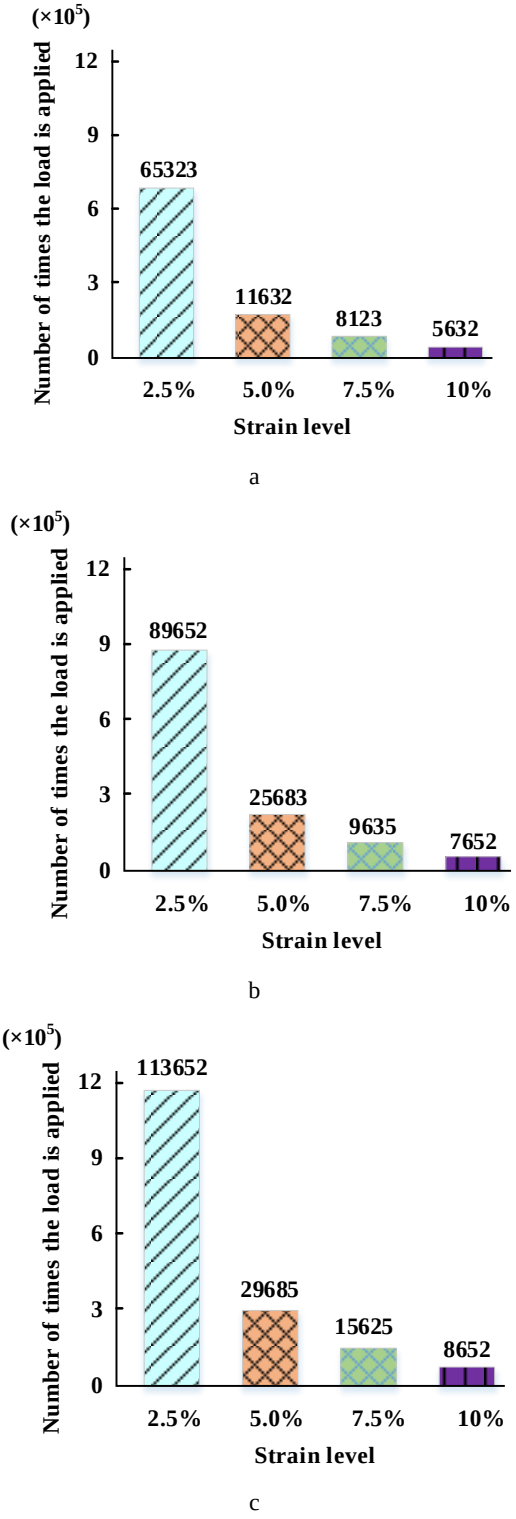

Fig. 9. The number of cycles in which fatigue failure occurs for three types of samples: a – sample 1; b – sample 2; c – sample 3

This dynamic energy absorption mechanism significantly reduces stress concentration inside the asphalt matrix, suppresses the initiation of microcracks, and delays the propagation speed of existing micro defects. The graphitized lamella and the sulfur cross-linked network of rubber powder work together to form a dual anti-aging system of "external shielding and internal buffering", thereby improving the anti-aging and anti-fatigue properties of modified asphalt.

Sample 3 showed the best anti-aging performance in the DSR test, its phase angle decreased by only 3.7°, while sample 1 and sample 2 decreased by 9.8° and 11.4°. This is because the high graphitization layer first forms a parallel arranged barrier network in the asphalt, delaying the diffusion rate of oxygen molecules. The conclusion of Idisi et al. indicates that when the interlayer spacing of graphene is less than 1 nm, the oxygen permeability can be reduced by two orders of magnitude [20], which is consistent with the result of the smallest viscosity reduction in sample 3. Secondly, rubber particles crosslinked with asphalt molecular chains through sulfur bonds, forming a 3D elastic network that absorbs internal stresses generated by thermal oxidative aging. The study by He et al. showed that when the rubber powder content is ≥ 3 %, it can significantly improve the elastic recovery rate of asphalt [21]. In this study, the composite system of rubber powder and graphene further optimized the network stability.

The fatigue cycle number of sample 3 under 10 % strain reached 8,652 times, significantly higher than that of sample 1 (5,632 times) and sample 2 (7,652 times). This advantage stemmed from the "rigid flexible interlocking" structure between graphene and rubber powder. The high modulus graphene layer enhanced the rigidity of the asphalt matrix and reduced viscous flow deformation through intercalation. Alghrafy et al. found that graphene can increase the complex modulus of asphalt, which is consistent with the results of this study. Rubber particles, as flexible phases, absorbed local stress concentration through deformation and suppressed microcrack propagation [22]. Compared with similar studies, Yue et al. found that the fatigue life of rubber powder modified asphalt can be increased by 2 – 3 times. In this study, the introduction of graphene further increased the number of cycles to 113,652 (2.5 % strain), indicating that the synergistic effect of the two is significantly better than that of a single modified system [23, 24].

4. CONCLUSIONS

This research aimed at the limitations of traditional modified asphalt in anti-aging, fatigue resistance, and environmental protection, and improved the performance of asphalt by adding graphene and rubber powder. In terms of anti-aging, graphene prepared by Hummers method has enhanced the interface bonding with asphalt due to its rich surface wrinkles and defects, effectively adsorbing light components and blocking oxygen diffusion; The elastic buffering effect of rubber powder further delayed the oxidation fracture of molecular chains, resulting in a decrease in the phase angle of the prepared G/RPCMA from 60.1° to 56.4° after 60 hours of aging, with the highest penetration retention rate (76.4 %). This shows that the prepared G/RPCMA has good anti-aging performance. At the same time, the aging indexes of carbonyl group and sulfoxide group of modified asphalt are 0.035 and 0.037 respectively, which are significantly lower than that of single component modified asphalt, showing excellent anti-

aging ability. In terms of fatigue resistance, the high graphitization degree of graphene forms a reinforced network to disperse stress, and rubber powder enhances material toughness. The two work together to optimize the viscoelastic balance, resulting in a lower modulus (0.9 kPa) of composite asphalt at low strain and a longer fatigue life at high strain. At a strain level of 2.5 %, the number of cycles reached 113652, and the attenuation rate was reduced by 31.2 % compared to the benchmark asphalt. The above results show that the prepared G/RPCMA has significant anti-aging and anti-fatigue synergistic properties. The synergistic mechanism originates from the three-dimensional network constructed by the physical barrier of graphene and the elastic recovery of rubber powder, which significantly inhibits aging hardening and delays the accumulation of fatigue damage. However, the experiment only simulates 5 – 10 years of natural aging and lacks long-term durability data on the coupling effects of multiple factors such as ultraviolet radiation and freeze-thaw cycles in real environments. Subsequent research will design a comprehensive aging experiment of UV humid heat freeze-thaw cycle, combined with molecular dynamics simulation to predict the lifespan of materials under extreme weather conditions.

REFERENCES

1. **Moraes, R., Yin, F., Chen, C., Andriescu, A., Mensching, D.J., Tran, N.** Evaluation of Long-Term Oven Aging Protocols on Field Cracking Performance of Asphalt Binders Containing Reclaimed Asphaltic Materials (Rap/Ras) *Road Materials and Pavement Design* 24 (1) 2023: pp. 437 – 450. https://doi.org/10.1080/14680629.2023.2181004
2. **Steinwolf, A.** Random Vibration Testing with Specified Fatigue Damage Spectrum and Preserved Power Spectral Density *Experimental Techniques* 49 (3) 2025: pp. 371 – 382. https://doi.10.1007/s40799-024-00748-3
3. **Wang, D., Wei, J., Zheng, S,Y.** Study of the Fatigue Damage Characteristics of Emulsified Asphalt Mastics *Journal of Materials in Civil Engineering* 36 (11) 2024: pp. 12 – 13. https://doi.10.1061/JMCEE7.MTENG-18009
4. **Cristache, A., Răcănel, C., Burlacu, A.** The Use of High-Performance Asphalt Mixtures in Heavy Traffic Road Structures *IOP Conference Series: Earth and Environmental Science* 664 (1) 2021: pp. 012094 – 012100. https://doi.org/10.1088/1755-1315/664/1/012094
5. **Yang, S., Zhu, H., Yang, X., Tan, Q., He, C.** Study on the Properties of Titanate Coupling Agent, Modified Heavy Calcium Carbonate, and Sbs Composite Modified Asphalt *Journal of Materials in Civil Engineering* 36 (6) 2024: pp. 10 – 11. https://doi.org/10.1061/JMCEE7.MTENG-17517
6. **Yan, K., Shi, K., Wang, M., Li, Q., Shi, J.** Performance of Nano-Tio2/Graphene Composite Modified Asphalt *Journal of Materials in Civil Engineering* 35 (11) 2023: pp. 12 – 13. https://doi.org/10.1061/JMCEE7.MTENG-15897
7. **Li, Z., Guo, T., Chen, Y., Liu, Q., Chen, Y.** The Properties of Nano-$CaCO_3$/Nano-ZnO/SBR Composite-Modified Asphalt *Nanotechnology Reviews* 10 (1) 2021: pp. 1253 – 1265. https://doi.org/10.1515/ntrev-2021-0082
8. **Wen, Y., Guo, N., Wang, L., Jin, X., Li, W., Wen, H.** Assessment of Various Fatigue Life Indicators and Fatigue Properties of Rock Asphalt Composite *Construction and Building Materials* 289 2021: pp. 123147. https://doi.org/10.1016/j.conbuildmat.2021.123147
9. **Wang, Q., Yu, R., Cai, L., Chen, X., Zhu, X., Xiao, Y., Zhang, X., Zhou, X., Fang, C.** Aging Resistance of Polyurethane/Graphene Oxide Composite Modified Asphalt: Performance Evaluation and Molecular Dynamics Simulation *Molecular Simulation* 49 (3) 2023: pp. 298 – 313. https://doi.org/10.1080/08927022.2022.2159052
10. **Yin, D., Wang, L., Yin, L., Wang, Z., Liu, S., Li, L.** Torsional Shear Resistance of Pavement Structure with Rubber Powder-Modified Asphalt Gravel Bonding Layer *Journal of Materials in Civil Engineering* 37 (4) 2025: pp. 25 – 30. https://doi.org/10.1061/JMCEE7.MTENG-18946
11. **Si, J., Shao, X., Li, J., Ma, H., Wang, J., Ruan, W., Yu, X.** Exploiting Graphene Oxide as a Potential Additive to Improve the Performance of Cold-Mixed Epoxy Asphalt Binder *Journal of Vinyl \& Additive Technology* 29 (3) 2023: pp. 482 – 492. https://doi.org/10.1002/vnl.21996
12. **Hoang, H.G.T., Nguyen, H.L., Tran, N.H., Ly, H.B.** Evaluation of the Influence of Graphene Oxide on Asphalt Binder Physical and Rheological Properties *Proceedings of the Institution of Mechanical Engineers Part L-Journal of Materials-Design and Applications* 238 (1) 2024: pp. 133 – 147. https://doi.org/10.1177/14644207231186610
13. **Lin, M., Lei, Y., Li, P., Wang, Z.L.** Study on the Rheological Properties and Modification Mechanism of Graphene/Rubber Composite-Modified Asphalt *Advances in Civil Engineering Materials* 14 (1) 2025: pp. 1 – 22. https://doi.org/10.1520/ACEM20230104
14. **Shamami, K.G., Effati, M., Mirabdolazimi, S.M.** Evaluation of the Effects of Graphene-Nanoplatelets on the Rutting, Fatigue Performance, and Moisture Sensitivity of Hot-Mix Asphalt *International Journal of Pavement Research and Technology* 18 (1) 2025: pp. 199 – 212. https://doi.org/10.1007/s42947-023-00337-4
15. **Ibrahim, A.H., Abbas, Y.M., Ayoub, H.A., Ali, M.H., Aldoori, M.** Novel Synthesis of Stabilized Bi1-X-yGdxDyyO1.5 Solid Electrolytes with Enhanced Conductivity for Intermediate Temperature Solid Oxide Fuel Cells (SOFCs) *Journal of Rare Earths* 42 (10) 2024: pp. 1903 – 1911. https://doi.org/10.1016/j.jre.2023.10.003
16. **Yin, Y., Dai, H., Yu, S., Bi, L., Traversa, E.** Tailoring Cobalt-Free $La_{0.5}Sr_{0.5}FeO_{3-\delta}$ Cathode with a Nonmetal Cation-Doping Strategy for High-Performance Proton-Conducting Solid Oxide Fuel Cells *Susmat* 2 (5) 2022: pp. 607 – 616. https://doi.org/10.1002/sus2.79
17. **Jiang, S., Qiu, H., Xu, S., Xu, X., Jiang, J., Xiao, B., Juliao, P.S.B., Su, C., Chen, D., Zhou, W.** Investigation and Optimization of High-Valent Ta-Doped $SrFeO_{3-\delta}$ as Air Electrode for Intermediate-Temperature Solid Oxide Fuel Cells *International Journal of Minerals Metallurgy and Materials* 31 (9) 2024: pp. 2102 – 2109. https://doi.org/10.1007/s12613-024-2872-1
18. **Gou, Y., Li, G., Ren, R., Xu, C., Qiao, J., Sun, W., Sun, K., Wang, Z.** Pr-Doping Motivating the Phase Transformation of the $BaFeO_{3-\delta}$ Perovskite as a High-Performance Solid Oxide Fuel Cell Cathode *ACS Applied Materials & Interfaces* 13 (17) 2021: pp. 20174 – 20184.

https://doi.org/10.1021/acsami.1c03514

19. **Yu, H., Shang, Y., Hu, Y., Pei, L., Zhang, G.** Transport Property of Wrinkled Graphene Nanoribbon Tuned by Spin-Polarized Gate Made of Vanadium-Benzene Nanowire *Nanomaterials* 13 (15) 2023: pp. 14 – 15. https://doi.org/10.3390/nano13152270
20. **Idisi, D.O., Benecha, E.M., Mwakikunga, B., Asante, J.K.O.** Effect of Interlayer Spacing on the Electronic and Optical Properties of SnS_2/Graphene/SnS_2 Sandwich Heterostructure: A Density Functional Theory Study *Journal of Computational Electronics* 23 (5) 2024: pp. 1029 – 1038. https://doi.org/10.1007/s10825-024-02202-4
21. **He, L., Chen, M., Tan, Y., Zhao, Z., Hu, Y., Zhao, M.** Evaluation of the Viscoelastic Characteristic of Asphalt Binder with Dry-Wet Cycle Aging *Journal of Materials in Civil Engineering* 36 (6) 2024: pp. 9 – 10. https://doi.org/10.1061/JMCEE7.MTENG-17313
22. **Alghrafy, Y., El-Badawy, S., Abd Alla, E.S.M.** A Comparative Study of Different Complex Shear Modulus Master Curve Techniques for Sulfur Extended Asphalt Modified with Recycled Polyethylene Waste *International Journal of Pavement Research and Technology* 15 (5) 2022: pp. 1023 – 1050. https://doi.org/10.1007/s42947-021-00070-w
23. **Yue, M., Yue, J., Wang, R., Guo, Y., Ma, X.** A Comprehensive Analysis of Fatigue and Healing Capacity of Sasobit Polymer-Modified Asphalt from Two Perspectives: Binder and Fam *Journal of Materials in Civil Engineering* 35 (3) 2023: pp. 19 – 20. https://doi.org/10.1061/(ASCE)MT.1943-5533.0004655